**RESEARCH ARTICLE**

**Thermodynamics and Molecular-Scale Phenomena**

# CO$_2$ solubility in aqueous *N*-methylcyclohexylamine (MCA) and *N*-cyclohexyl-1,3-propanediamine (CHAP) solutions

Fragkiskos Tzirakis[1,2] ⓘ | Athanasios I. Papadopoulos[2] | Panos Seferlis[2,3] | Ioannis Tsivintzelis[1] ⓘ

[1]Department of Chemical Engineering, Aristotle University of Thessaloniki, Thessaloniki, Greece

[2]Chemical Process and Energy Resources Institute, Centre for Research and Technology-Hellas, Thessaloniki, Greece

[3]Department of Mechanical Engineering, Aristotle University of Thessaloniki, Thessaloniki, Greece

**Correspondence**
Fragkiskos Tzirakis and Ioannis Tsivintzelis, Department of Chemical Engineering, Aristotle University of Thessaloniki, Thessaloniki 54124, Greece.
Email: tzirakis@certh.gr and tioannis@cheng.auth.gr

**Abstract**

*N*-methylcyclohexylamine (MCA) and *N*-cyclohexyl-1,3-propanediamine (CHAP) have been suggested, in mixtures with lipophilic amines, as potential phase change solvents for CO$_2$ capture applications, and subsequently studied as promising alternatives to monoethanolamine (MEA) for minimizing the desorber's energy requirements. In this study, new high pressure experimental data were obtained for the solubility of CO$_2$ in aqueous solutions containing MCA or CHAP at 313 and 333 K. The obtained data were used to parameterize the modified Kent–Eisenberg model. In this direction, CHAP was modeled assuming a "principle of independent reactivity," that is, that the reactivity of each amine group does not depend on the potential reaction of the other one. It was shown that through this approach the model can be successfully applied to diamines using the relevant equations of amine mixtures.

**KEYWORDS**
amine solutions, CHAP, CO$_2$ capture, Kent–Eisenberg model, MCA, phase equilibria

## 1 | INTRODUCTION

For post-combustion CO$_2$ capture many research activities are underway at present. These include solid sorbents, membranes, and new liquid absorbents.[1] Among such technologies, absorption/desorption processes have received significant attention, with several efforts observed worldwide regarding the scaling-up of capture plants.[2] The major limitation of such processes is the reboiler duty required for solvent regeneration, which poses significant energy penalties in the CO$_2$ emitting plants. To reduce the energy costs of absorption/desorption systems, it is imperative to search for solvents that can decrease the heat duty in the order of 2.0 GJ/ton of CO$_2$ captured or below.[2]

In this direction, numerous different solvents have been investigated at laboratory or pilot scale,[3,4] but few have been tested at larger capacity

units. Among such solvents, mixtures such as 2-amino-2-methyl-1-propanol (AMP) and piperazine (PZ), methyldiethanolamine (MDEA) and PZ, or the proprietary solvent KS-1 appear to be promising as they indicated potential for regeneration energy around 3.0 GJ/ton of CO$_2$ captured, compared to the approximately 4.0 GJ/ton of CO$_2$ captured with the 30 wt.% MEA.[5,6] While these reductions have been attained in standard absorption/desorption flowsheets, solvents such as PZ exhibited reductions down to approximately 2.0 GJ/ton CO$_2$ in flowsheets that included internal energy recovery equipment.[2]

Recently, using computer aided molecular design (CAMD) coupled with Pareto optimization, Papadopoulos et al.[7] suggested *N*-cyclohexyl-1,3-propanediamine (CHAP) as a novel promising solvent. Aqueous *N*-cyclohexyl-1,3-propanediamine (CHAP)—*N,N*-dimethyl-cyclohexylamine (DMCA) mixtures were investigated and it was shown that they exhibit high cyclic capacity and low regeneration

energy requirements, around 2.3 GJ/ton of captured $CO_2$. These mixtures exhibit phase-change behavior, in which a second liquid phase is generated upon a change in processing conditions.[8] The second liquid phase is lean in $CO_2$ and may be recycled directly to the absorber, thus enabling a reduction of the regeneration energy requirements due to the reduction of the $CO_2$-rich solvent that is thermally processed in the desorber. Phase-change solvents do not require additional equipment, other than a simple decanter. In a previous study,[9] it was indicated that mixtures of cyclohexylamines, such as *N*-methylcyclohexylamine (MCA) and DMCA, can reduce the regeneration energy in the range of 2.0–2.5 GJ/ton $CO_2$. Another work[10] further showed that MCA and CHAP/DMCA can result in up to 47% lower operating costs than MEA.

In this work, new experimental data and modeling results are presented for aqueous solutions of MCA and CHAP, since both were used in mixtures with DMCA as phase change solvents for $CO_2$ capture applications. The available literature data regarding the phase behavior of systems containing MCA, CHAP and their mixtures under $CO_2$ atmosphere are shown in Table 1.

In more detail, Perdomo et al.[11] presented experimental equilibrium results for DMCA and MCA aqueous solutions at $CO_2$ partial pressures up to approximately 80 kPa. It was shown that at MCA aqueous solutions, although biphasic in the absence of $CO_2$ and at ambient conditions, present a single liquid phase upon $CO_2$ dissolution at 40 and 60°C and for $CO_2$ partial pressures higher than approximately 15 kPa. At 90°C, they present liquid–liquid phase separation for $CO_2$ partial pressures lower than approximately 25 kPa, while they present a single liquid phase for high loading conditions (higher $CO_2$ partial pressures). The results were modeled using the SAFT-γ Mie group contribution approach.[11]

The $CO_2$-DMCA-CHAP-$H_2O$ system was experimentally investigated at 40–90°C, using an aqueous amine solution with total amine content of 44.3 wt.%, (app. 3 M) at a 2:1 DMCA to CHAP mole ratio.[13] It was shown that upon liquid–liquid phase separation, the hydrophilic CHAP is accumulated in the $CO_2$ rich aqueous phase, while the hydrophobic DMCA is mainly found in the organic, $CO_2$ lean, phase. In addition, it was concluded that as the $CO_2$ partial pressure increases, more amine molecules, and mainly the lipophilic DMCA, are transformed in hydrophilic ionic species that end up in the aqueous phase.[13]

Another work[15] investigated aqueous solutions of DMCA-MCA blends. The $CO_2$ solubility in the aqueous DMCA-MCA blends is high and significantly increases with the ratio of MCA in the amine mixture. Using NMR and theoretical analyses, the authors showed that the formed MCA carbamate is relatively unstable and it is easily transformed to bicarbonate, rendering bicarbonate as the main product. Finally, the regeneration energy of such aqueous solvent is very low and in the range of 2.3 GJ/ton $CO_2$. Considering such phase change solvents, another study[17] applied NMR analysis and quantum calculations revealing the mechanism of $CO_2$ absorption. The performed analysis proved the occurrence of a two-stage interaction mechanism; the first stage was controlled by absorption kinetics, and the second stage was controlled by thermodynamics.

**TABLE 1** Literature studies reporting experimental data for the $CO_2$ loading and the phase behavior of aqueous solvents containing MCA or CHAP

| Amine(s) | References |
| --- | --- |
| CHAP[a] | Papadopoulos et al.[7] |
| MCA | Zhang[9]; Perdomo et al.,[11] Jeon et al.[12] |
| DMCA + CHAP[a] | Papadopoulos et al.[7]; Tzirakis et al.[13] |
| DMCA + MCA | Tzirakis et al.[14]; Wang et al.[15]; Zhang[9] |
| Screening experiments | Ye et al.[16] |

[a]Mentioned as S₁N in Papadopoulos et al.[7]

The rigorous thermodynamic modeling of the vapor–liquid equilibrium of aqueous amine systems under $CO_2$ atmosphere requires accounting for all ionic and intermolecular interactions in the liquid solution and the calculation of fugacities in both phases. This is usually performed using electrolyte equation of state (EoS) theories, or *EoS/$G^E$* models, considering also the equilibrium constants of all relevant chemical reactions.[18–20] Such approach, although rigorous, presents significant complexity and, consequently, several simplifications are often applied, for example, ionic interactions are not explicitly accounted for and are lumped into the hydrogen bonding term of the relevant *EoS* models.[7,21–24]

The thermodynamic approaches for modeling gas solubility in such systems were reviewed recently.[20] It was observed that several empirical or semi-empirical approaches which are considerably simpler than EoS models, present a good correlation and prediction ability. In this direction, the most popular one is the Kent–Eisenberg model,[25] which requires the knowledge of equilibrium constants of all chemical reactions, and Henry's constant for calculating the molecular $CO_2$ dissolution into the liquid phase. Kent and Eisenberg[25] used the literature values of ionization and Henry's law constants, except from those referring to the amine reactions (the amine ionization reaction and the carbamate hydrolysis one), which were fitted to the experimental solubility data. According to Jou et al.,[26] in this way all nonidealities of the system are absorbed by the effective values of the adjustable parameters. Due to its low computational complexity, the model found numerous applications in correlating the $CO_2$ and $H_2S$ solubility in aqueous amine systems and several modifications were presented in published literature.[27]

Based on previous works,[7,10] it is deemed interesting to examine further MCA and CHAP aqueous solutions. This is due to their excellent carbon capture capabilities and phase change behavior when blended with DMCA. In this study we use a pressure decay method to obtain new experimental data for the $CO_2$ loading of aqueous MCA and CHAP solutions. The new experimental data cover a wide range of pressures, in contrast with the existing data presented in Table 1, which are limited to low pressures. Thus, the obtained new data allow the rigorous parameterization of the modified Kent–Eisenberg model that was extended to systems containing diamines with both a carbamate- and a non-carbamate forming amine group.

## 2 | EXPERIMENTAL

### 2.1 | Materials

The materials used in this work are shown in Table 2. They are used as received without further purification. The molecular structure of both investigated amines is shown in Figure 1.

### 2.2 | Experimental apparatus and procedure

The $CO_2$ solubility in aqueous MCA and CHAP solutions was measured using a pressure decay method and a relevant apparatus that is shown in Figure 2. The experimental procedure is described in our previous works.[23,24] Briefly, the air is removed from the high-pressure cell and, subsequently, a known amount of the aqueous solvent (around 25 g, maximum error ±0.002 g) is added. Then, 3–5 g of $CO_2$, depending on the experiment, are added to the system. The added amount of $CO_2$ is estimated (maximum error ± 0.002 g) by measuring the mass (accuracy of ±0.001 g) of a high-pressure $CO_2$ containing flask, before and after the addition. The pressure and the temperature inside the equilibrium cell are continuously monitored, using a pressure transducer (WIKA A-10, ±0.5%) and a Pt-100 (±0.01 K) thermometer, respectively. It is assumed that equilibrium conditions are reached upon pressure stabilization for at least 1 h. Knowing the temperature and pressure conditions, as well as the volume of the vapor phase, the amount of the absorbed $CO_2$ is calculated using the mass balance equations.[23,24] The equilibrium high-pressure cell is immersed inside a water bath of constant temperature (stability of temperature in the bath equal to 0.1 K). As described previously,[24] the volume of the cell (152.2 ± 1.6 cm$^3$ at 298.15 K) was estimated at various temperatures by measuring the pressure after the addition of known $CO_2$ amounts. In all experimental conditions, the needed $CO_2$ densities were obtained from NIST.[28]

According to such experimental procedure,[23,24] the total pressure of the system is measured. In order to estimate the partial pressure of $CO_2$, the vapor pressure of the aqueous solution is subtracted from the total pressure. Since the investigated solutions are not volatile, such approximation, which is often used in similar studies,[29,30] results in an insignificant correction, especially at relatively high pressures. In all cases, the uncertainties in the reported values for the $CO_2$ loading denote the maximum error, estimated through a propagation of errors analysis, knowing the uncertainties of all experimental measurements (i.e., weight of the materials, volume of the cell, etc.).[24]

### 2.3 | A modified Kent–Eisenberg model

A modified Kent–Eisenberg model was used in this study to correlate the experimental data as shown next in this section. In contrast with the original model,[25] equations are not solved iteratively, but a polynomial equation is used for estimating the hydrogen ion concentration, as shown by Haji-Sulaiman et al.[31]

Although the relevant equations of such modified Kent–Eisenberg model for pure carbamate or non-carbamate forming amines are presented in many studies,[27,31] the relevant equations and
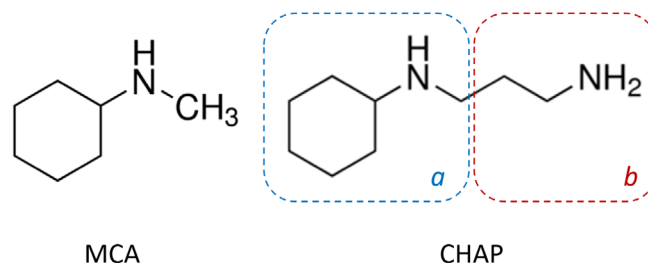


**FIGURE 1**  Molecular structure of *N*-methyl-cyclohexylamine (MCA) and *N*-cyclohexyl-1,3-propanediamine (CHAP), which consists of a secondary (*a*) and a primary amine group (*b*) part, with the secondary amine group part (*a*) resembling the structure of MCA.
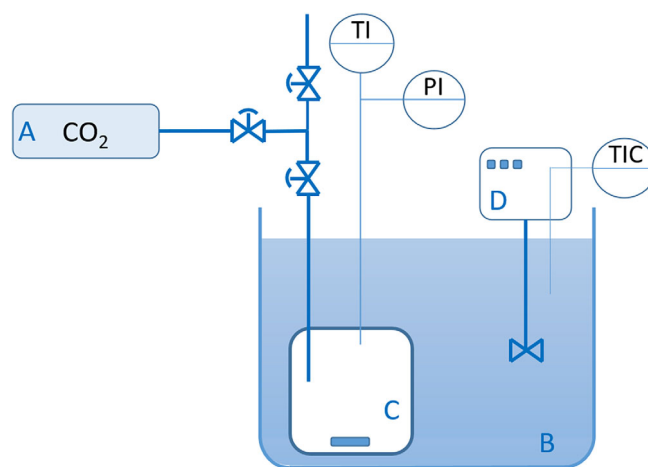


**FIGURE 2**  Experimental apparatus for VLE measurements consisting of a $CO_2$ gas flask (A), water bath (B), equilibrium high-pressure cell (C), magnetically stirred and equipped with temperature and pressure sensors, and temperature controller (D).
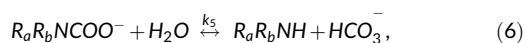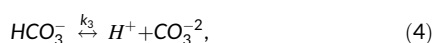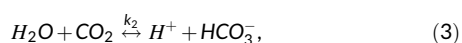
**TABLE 2**  Chemicals used in this work

| Product name | Abbreviation | CAS-number | Purity | Supplier |
|---|---|---|---|---|
| Carbon dioxide | $CO_2$ | 124-38-9 | 99.9 (vol%) | Air Liquide |
| Nitrogen | $N_2$ | 7727-37-9 | 99.9 (vol%) | Air Liquide |
| Helium | He | 7440-59-7 | 99.99 (vol%) | Air Liquide |
| *N*-methylcyclohexylamine | MCA | 100-60-7 | 99% | Sigma Aldrich |
| *N*-cyclohexyl-1,3-propanediamine | CHAP | 3312-60-5 | 98% | ITC |

approaches for mixtures are not always well documented. Suleman et al.[27] recently reviewed the use of such models and approaches in literature and mention three possible ways of developing a model for amine blends. According to the first and most simple approach, but also the most approximate one, the single amine models are solved and the resulting $CO_2$ solubilities in both single amine solutions are summed up to estimate the solubility in the blend. According to the second one, the polynomial equations of the single amine models (that are used for estimating the hydrogen ion concentration) are summed up and then the loading is estimated through a combined equation. However, the summation of such polynomial equations adds unnecessary empiricism to the model. Finally, according to the third and most rigorous one, the mass and charge balances for the multicomponent system are thoroughly set, resulting in a rigorous polynomial equation for the hydrogen ion concentration. According to this work,[27] all approaches result in similar estimations for the $CO_2$ solubility, despite that the first two of them are very approximate.

In this study, the third approach, as described by Suleman et al.,[27] is followed and the relevant equations are presented for a mixture of a carbamate forming amine ($R_aR_bNH$) and a non-carbamate forming amine ($R_cR_dNH$), that, as we will show, can be also used for diamines.

Assuming a mixture of a carbamate forming amine ($R_aR_bNH$) and a non-carbamate forming amine ($R_cR_dNH$), we can write the following chemical reactions and the relevant equilibrium constants[27,31]:

$$R_aR_bNH_2^+ \overset{k_{11}}{\leftrightarrow} R_aR_bNH + H^+, \tag{1}$$

$$R_cR_dNH_2^+ \overset{k_{12}}{\leftrightarrow} R_cR_dNH + H^+, \tag{2}$$

$$H_2O + CO_2 \overset{k_2}{\leftrightarrow} H^+ + HCO_3^-, \tag{3}$$

$$HCO_3^- \overset{k_3}{\leftrightarrow} H^+ + CO_3^{-2}, \tag{4}$$

$$H_2O \overset{k_4}{\leftrightarrow} H^+ + OH^-, \tag{5}$$

$$R_aR_bNCOO^- + H_2O \overset{k_5}{\leftrightarrow} R_aR_bNH + HCO_3^-, \tag{6}$$
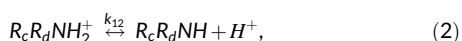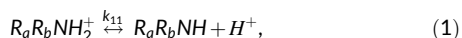
where $R_aR_bNH_2^+$ and $R_cR_dNH_2^+$ are the protonated forms of the carbamate forming and the non-carbamate forming alkanolamine, respectively, while $R_aR_bNCOO^-$ represents the carbamate anion.

The equilibrium constants for Equations 1–6 are written as follows[27]:

$$\text{Alkanolamine deprotonation}: k_{11} = [R_aR_bNH][H^+]/[R_aR_bNH_2^+], \tag{7}$$

$$\text{Alkanolamine deprotonation}: k_{12} = [R_cR_dNH][H^+]/[R_cR_dNH_2^+], \tag{8}$$

$$\text{Bicarbonate formation}: k_2 = [HCO_3^-][H^+]/[CO_2], \tag{9}$$

$$\text{Carbonate formation}: k_3 = [CO_3^{-2}][H^+]/[HCO_3^-], \tag{10}$$

$$\text{Water dissociation}: k_4 = [OH^-][H^+], \tag{11}$$

$$\text{Carbamate hydrolysis}: k_5 = [R_aR_bNH][HCO_3^-]/[R_aR_bNCOO^-]. \tag{12}$$

Equations (7)–(12) result in the following equations for the concentration of species:

$$[OH^-] = k_4/[H^+], \tag{13}$$

$$[HCO_3^-] = k_2[CO_2]/[H^+], \tag{14}$$

$$[CO_3^{-2}] = k_2k_3[CO_2]/[H^+]^2, \tag{15}$$

$$[RRNCOO^-] = k_{11}k_2[CO_2][R_aR_bNH_2^+]/\left(k_5[H^+]^2\right). \tag{16}$$

Moreover, we can write three mass balance equations and one for the charge balance of the solution.

*Alkanolamine balances*:

$$[R_aR_bNHtot] = [R_aR_bNH] + [R_aR_bNH_2^+] + [RRNCOO^-], \tag{17}$$

$$[R_cR_dNHtot] = [R_cR_dNH] + [R_cR_dNH_2^+], \tag{18}$$

$$[RRNHtot] = [R_aR_bNHtot] + [R_cR_dNHtot]. \tag{19}$$

*Carbon dioxide balance*:

$$a[RRNHtot] = [CO_2] + [HCO_3^-] + [CO_3^{-2}] + [RRNCOO^-]. \tag{20}$$

*Charge balance*:

$$[H^+] + [R_aR_bNH_2^+] + [R_cR_dNH_2^+] = [OH^-] + [HCO_3^-] + 2[CO_3^{-2}] + [RRNCOO^-], \tag{21}$$

where $\alpha$ is the carbon dioxide loading (expressed as mole of $CO_2$ per mole of amine), $[RRNHtot]$ is the total concentration of amines and $[CO_2]$ is the liquid phase carbon dioxide solubility, determined by Henry's law, as follows:

$$[CO_2] = P_{CO2}/H_{CO2}, \tag{22}$$

where $P_{CO2}$ and $H_{CO2}$ are the $CO_2$ partial pressure in the vapor phase and the Henry's constant, respectively.

For a mixture of a carbamate and a non-carbamate forming alkanolamine, Equations (7)–(21) reduce to a system of three equations with three unknowns, $[H^+]$, $[R_aR_bNH_2^+]$ and $[R_cR_dNH_2^+]$, as follows:

**TABLE 3**  Parameters of Equation (26)

| Parameters | Relation |
| --- | --- |
| $A$ | $-k_5$ |
| $B$ | $-k_5[R_aR_bNH_{tot}] - k_5[R_cR_dNH_{tot}] - k_{11}k_5 - k_{12}k_5$ |
| $C$ | $-k_{12}k_5[R_aR_bNH_{tot}] - k_{11}k_5[R_cR_dNH_{tot}] + k_4k_5 + k_2k_5[CO_2] - k_{11}k_2[CO_2] - k_{11}k_{12}k_5$ |
| $D$ | $k_{11}k_2[R_aR_bNH_{tot}][CO_2] - k_{11}k_2[R_cR_dNH_{tot}][CO_2] + 2k_2k_3k_5[CO_2] + k_{11}k_4k_5 + k_{11}k_2k_5[CO_2] - k_{11}k_{12}k_2[CO_2] + k_{12}k_4k_5 + k_{12}k_2k_5[CO_2]$ |
| $E$ | $k_{11}k_{12}k_2[R_aR_bNH_{tot}][CO_2] + 2k_{11}k_2k_3k_5[CO_2] + k_{11}k_2k_4[CO_2] + k_{11}k_2^2[CO_2]^2 + 2k_{12}k_2k_3k_5[CO_2] + k_{11}k_{12}k_4k_5 + k_{11}k_{12}k_2k_5[CO_2]$ |
| $F$ | $2k_{11}k_2^2k_3[CO_2]^2 + k_{11}k_{12}k_2k_4[CO_2] + k_{11}k_{12}k_2^2[CO_2]^2 + 2k_{11}k_{12}k_2k_3k_5[CO_2]$ |
| $G$ | $2k_{11}k_{12}k_2^2k_3[CO_2]^2$ |

$$[R_aR_bNH_{tot}] = \left(1 + k_{11}/[H^+] + k_{11}k_2[CO_2]/\left(k_5[H^+]^2\right)\right)[R_aR_bNH_2^+], \tag{23}$$

$$[R_cR_dNH_{tot}] = (1 + k_{12}/[H^+])[R_cR_dNH_2^+], \tag{24}$$

$$[R_aR_bNH_2^+]\left(1 - k_{11}k_2[CO_2]/\left(k_5[H^+]^2\right)\right) + [R_cR_dNH_2^+]$$
$$= k_4/[H^+] + k_2[CO_2]/[H^+] + 2k_2k_3[CO_2]/[H^+]^2 - [H^+]. \tag{25}$$

After some algebra, the following polynomial equation of 6th order is obtained:

$$A[H^+]^6 + B[H^+]^5 + C[H^+]^4 + D[H^+]^3 + E[H^+]^2 + F[H^+] + G = 0, \tag{26}$$

where $A$, $B$, $C$, $D$, $E$, $F$ and $G$ are shown in Table 3.

Only the root with physical meaning, that is, $pH \in [7, 12]$,[27,31] is kept from Equation (26), while the loading is calculated through the following equations:

$$\alpha = \left([CO_2] + \frac{k_2[CO_2]}{[H^+]} + \frac{k_2k_3[CO_2]}{[H^+]^2} + [RRNCOO^-]\right)/([RRNHtot]), \tag{27}$$

where

$$[RRNCOO^-] = (k_{11}k_2[CO_2][R_aR_bNH_{tot}])/\left(k_5[H^+]^2 + k_{11}k_5[H^+] + k_{11}k_2[CO_2]\right). \tag{28}$$

The above equations are sufficient for estimating the loading in any mixture of two amines, one carbamate forming and one non-carbamate forming one. If two different monoamines are considered, then their total concentrations, $[R_aR_bNHtot]$ and $[R_cR_dNHtot]$, refer to the initial composition of the unloaded aqueous solvent (i.e., denote moles of amine molecules in kg of water). Similarly, all other species concentrations refer to moles of molecules (or ions) per kg of water and the calculated loading through Equation (27) denotes the moles of absorbed $CO_2$ per mole of amine molecules.

However, CHAP is a diamine consisting of two amine groups (Figure 1), one that is sterically hindered, and, thus, considered as non-carbamate forming group, and one carbamate forming group. In

such case, one can also use the aforementioned equations. However, in that case all amine species concentrations will denote moles of amine groups and not moles of molecules. In that case the calculated loading from Equation (27) denotes the moles of absorbed $CO_2$ per mole of amine groups (not molecules) and should be adequately converted to be compared to experimental data (which usually present loadings as moles of $CO_2$ per mole of amine molecules).

In case of MCA (Figure 1), which has a single amine (assumed as sterically hindered and, thus, non-carbamate forming) group in each molecule, $[R_aR_bNH_{tot}]$ and $[R_aR_bNH_2^+]$ in Equations (23)–(25) are set equal to zero. Thus, the system of Equations (23)–(25) reduces to the following one:

$$[R_cR_dNH_{tot}] = (1 + k_{12}/[H^+])[R_cR_dNH_2^+], \tag{29}$$

$$[R_cR_dNH_2^+] = k_4/[H^+] + k_2[CO_2]/[H^+] + 2k_2k_3[CO_2]/[H^+]^2 - [H^+], \tag{30}$$

which after some algebra gives the following polynomial equation, as described in similar studies[27]:

$$A'[H^+]^4 + B'[H^+]^3 + C'[H^+]^2 + D'[H^+] + E' = 0, \tag{31}$$

where $A'$, $B'$, $C'$, $D'$ and $E'$ are shown in Table 4.

Also, by setting $[RRNCOO^-] = 0$, Equation (27) reduces to:

$$\alpha = \left([CO_2] + \frac{k_2[CO_2]}{[H^+]} + \frac{k_2k_3[CO_2]}{[H^+]^2}\right)/([R_cR_dNH_{tot}]). \tag{32}$$

The equilibrium constants, $k_i$ or $k_{ij}$, are estimated using empirical relations as follows[27]:

**TABLE 4**  Parameters[27] of Equation (31)

| Parameters | Relation |
| --- | --- |
| $A'$ | $1$ |
| $B'$ | $[R_cR_dNH_{tot}] + k_{12}$ |
| $C'$ | $-k_4 - k_2[CO_2]$ |
| $D'$ | $-k_{12}k_4 - 2k_2k_3[CO_2] - k_{12}k_2[CO_2]$ |
| $E'$ | $-2k_{12}k_2k_3[CO_2]$ |

$$\ln(k_i) = \frac{A_i}{T} + B_i \ln T + C_i T + D_i. \tag{33}$$

Details on the parameters that are fitted in Equation (33), are presented in the modeling results section.

# 3 | RESULTS AND DISCUSSION

## 3.1 | Experimental results

Considering the aqueous CHAP solution, measurements were performed at 313 and 333 K for $CO_2$ partial pressures higher than

**TABLE 5** Solubility of $CO_2$ in 32.5 ± 0.1 wt.% aqueous CHAP solution at 313 and 333 K

| Temperature/K[a] | $CO_2$ partial pressure[b], P/kPa | $CO_2$ loading, $\alpha$/mole $CO_2$ per mole of amine |
|---|---|---|
| 313.15 | 80 | 1.297 ± 0.043 |
| | 187 | 1.380 ± 0.043 |
| | 532 | 1.544 ± 0.047 |
| | 792 | 1.596 ± 0.050 |
| | 1207 | 1.676 ± 0.048 |
| | 1640 | 1.719 ± 0.054 |
| 333.15 | 141 | 1.231 ± 0.044 |
| | 276 | 1.293 ± 0.044 |
| | 680 | 1.417 ± 0.049 |
| | 963 | 1.467 ± 0.052 |
| | 1880 | 1.606 ± 0.056 |

[a]Standard uncertainty in temperature $u(T) = 0.10$ K.
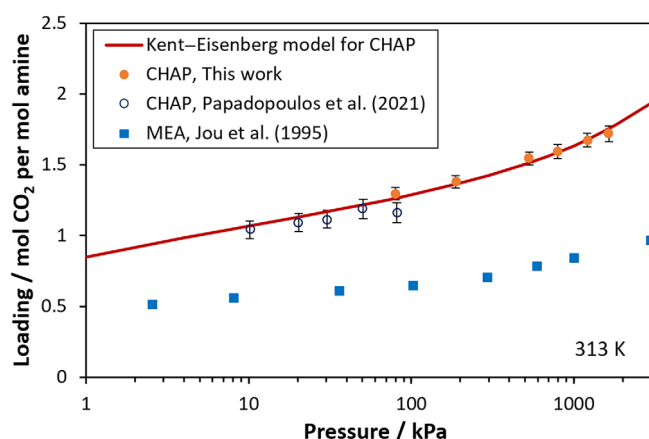[b]Standard uncertainty in total pressure $u(p) = 0.005 \cdot P$.



**FIGURE 3** Solubility of $CO_2$ in 32.5 wt.% aqueous CHAP solution at 313 K. Experimental data from this work (solid circles) and Papadopoulos et al.[7] (open circles) and model correlations (curve). Experimental data[30] for the $CO_2$ solubility in 30 wt.% aqueous MEA solution are also shown (solid squares) for comparison.
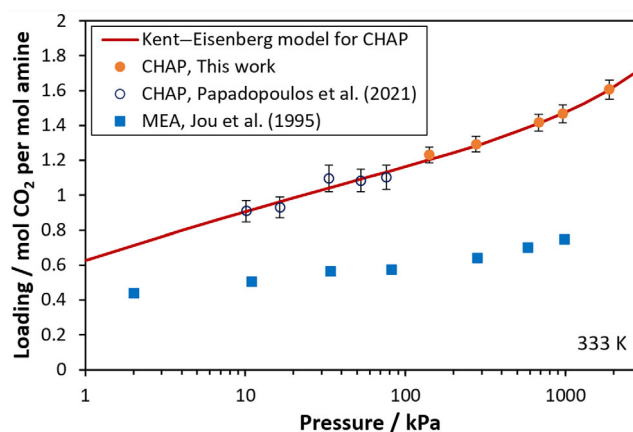


**FIGURE 4** Solubility of $CO_2$ in 32.5 wt.% aqueous CHAP solution at 333 K. Experimental data from this work (solid circles) and Papadopoulos et al.[7] (open circles) and model correlations (curve). Experimental data[30] for the $CO_2$ solubility in 30 wt.% aqueous MEA solutions are also shown (solid squares) for comparison.

**TABLE 6** Solubility of $CO_2$ in 31.5 ± 0.1 wt.% aqueous MCA solution at 313 and 333 K

| Temperature/K[a] | $CO_2$ partial pressure[b], P/kPa | $CO_2$ loading, $\alpha$/mole $CO_2$ per mole of amine |
|---|---|---|
| 313 | 114 | 0.963 ± 0.024 |
| | 132 | 0.973 ± 0.025 |
| | 180 | 0.975 ± 0.031 |
| | 291 | 0.988 ± 0.024 |
| | 311 | 0.991 ± 0.033 |
| | 412 | 1.003 ± 0.028 |
| | 447 | 0.996 ± 0.026 |
| | 547 | 1.009 ± 0.028 |
| | 763 | 1.016 ± 0.030 |
| | 988 | 1.069 ± 0.031 |
| | 1225 | 1.061 ± 0.035 |
| 333 | 52 | 0.849 ± 0.029 |
| | 166 | 0.935 ± 0.024 |
| | 178 | 0.948 ± 0.025 |
| | 221 | 0.951 ± 0.032 |
| | 342 | 0.970 ± 0.024 |
| | 354 | 0.972 ± 0.033 |
| | 459 | 0.990 ± 0.029 |
| | 493 | 0.987 ± 0.026 |
| | 597 | 1.001 ± 0.028 |
| | 821 | 1.013 ± 0.030 |
| | 1084 | 1.054 ± 0.031 |
| | 1324 | 1.055 ± 0.035 |

[a]Standard uncertainty in temperature $u(T) = 0.10$ K.
[b]Standard uncertainty in total pressure $u(p) = 0.005 \cdot P$.

80 kPa, since the pressure decay method is not recommended at very low pressures or high temperatures due to potential solvent vaporization. All measurements were performed starting for a 32.5 wt.% aqueous amine solution. The experimental results are presented in Table 5. The obtained data are compared with available literature low pressure data,[7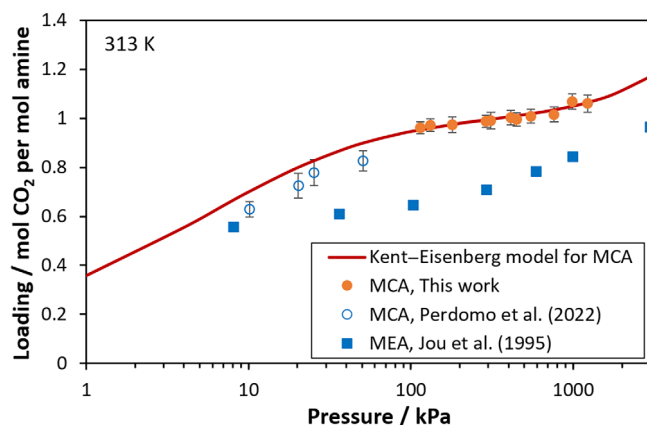] which were obtained using a chemical analysis experimental technique, in Figures 3 and 4. It is observed that both data sets are in very good agreement, despite the differences in the investigated pressure range. Furthermore, as shown in Figures 3 and 4, the investigated aqueous CHAP solution presents almost the double $CO_2$ solubility than 30 wt.% aqueous MEA solution, which is considered as a benchmark solvent, and which is currently used in $CO_2$ capture applications.

Considering the MCA aqueous system, measurements were performed at 313 and 333 K. All measurements were performed starting from a 31.5 wt.% aqueous amine solution. It was observed that aqueous MCA mixtures, although biphasic at temperatures higher than approximately 283 K (MCA-water presents liquid–liquid phase separation with lower critical solution temperature, LCST, behavior), present one liquid phase upon $CO_2$ dissolution at the investigated conditions. Thus, the $CO_2$ loaded aqueous MCA solutions present one liquid phase at 313 and 333 K at all the investigated $CO_2$ partial pressures.

The experimental results are presented in Table 6. The obtained data are compared with available low pressure literature data,[11] which were obtained using a chemical analysis experimental technique, in Figures 5 and 6. It is observed that both data sets are in very good agreement, despite the differences in the investigated pressure range. Moreover, as shown in Figures 5 and 6, the investigated MCA aqueous solution presents considerably higher $CO_2$ solubility than 30 wt.% aqueous MEA solution, which is considered as a benchmark solvent, and which is currently used in $CO_2$ capture applications.



**FIGURE 5** Solubility of $CO_2$ in aqueous MCA solution at 313 K. Experimental data from this work (solid circles) and Perdomo et al.[11] (open symbols)) and model correlations (curve). Experimental data[30] for the $CO_2$ solubility in 30 wt.% aqueous MEA solutions are also shown (solid squares) for comparison.
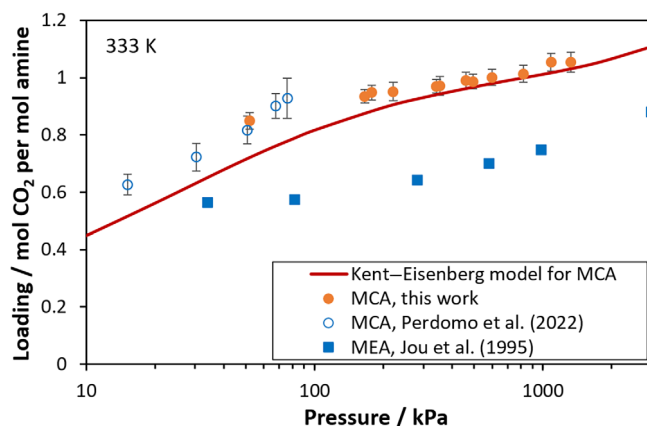
## 3.2 | Modeling results

In order to apply the modified Kent–Eisenberg model, one has to know the temperature dependence of all needed equilibrium constants of reactions (1)–(6) and the Henry's law constant (shown in Equation (22)), which is usually given through the empirical equation (33). The parameters of Equation (33) for the equilibrium constants of reactions (3)–(5), as well as the parameters for Henry's constant, are usually obtained from literature.[27] Such values, which were also used in this study, are presented in Table 7.

Non-sterically hindered primary or secondary amines, react with $CO_2$ mainly through the carbamate formation mechanism, which imposes a maximum loading, due to the stoichiometry of the reactions, equal to 0.5 mole of $CO_2$ per mole of amine.[33] On the other hand, sterically hindered amines react through a different mechanism, since the produced carbamate is relatively unstable, and may present



**FIGURE 6** Solubility of $CO_2$ in aqueous MCA solution at 333 K. Experimental data from this work (solid circles) and Perdomo et al.[11] (open symbols)) and model correlations (curve). Experimental data[30] for the $CO_2$ solubility in 30 wt.% aqueous MEA solutions are also shown (solid squares) for comparison.

**TABLE 7** Parameters of the empirical equation (33) obtained from literature[32]

| Parameter[a] (T in K) | Units | A | B | C | D |
|---|---|---|---|---|---|
| $H_{CO2}$ | atm kg/mol | −6789.04 | −11.4519 | −0.010454 | 94.4914 |
| $k_2$ | mol/kg | −12092.1 | −36.7816 | – | 235.482 |
| $k_3$ | mol/kg | −12431.7 | −35.4819 | – | 220.067 |
| $k_4$ | (mol/kg)$^2$ | −13445.9 | −22.4773 | – | 140.932 |

[a]Temperature validity: 273–498 K.

loadings around 1 mole of $CO_2$ per mole of amine, even at rather low $CO_2$ partial pressures.[33] However, the experimental loading may present higher values than such theoretical limits, especially at relatively high $CO_2$ partial pressures, due to molecular $CO_2$ dissolution and/or due to significant carbamate hydrolysis.

Thus, before the application of the Kent–Eisenberg model, one has to assume the appropriate mechanism for the investigated amine. In this study, MCA was modeled as a non-carbamate forming sterically hindered amine. Having in mind the aforementioned theoretical maximum loadings, such assumption is in line with the experimental loading values that are around 1 mole of $CO_2$ per mole of amine, as shown in Table 6, even at rather low pressures. Consequently, reactions (1) and (6) were not accounted for and the model was applied using Equations (31) and (32). The $k_{12}$ equilibrium constant for reaction (2) was given by Equation (33). The parameters of that equation were adjusted to the experimental data of this study and other literature data.[11] However, results showed that the use of more than one adjustable parameter in Equation (33) does not significantly improve the correlations. Consequently, only the parameter $A$ was estimated, while parameters $B$, $C$ and $D$ were kept equal to zero, as shown in Table 8. Here it is worth mentioning that if $B$ and $C$ parameters of Equation (33) are set equal to zero, such equation better resembles the Arrhenius equation and unnecessary empiricism is avoided. Therefore, using only one adjustable parameter, the model rather satisfactorily correlates the experimental data, presenting an average absolute deviation equal to 5.5% from the experimental data of this work and the data of Perdomo et al.[11] (for 313, 333, and 363 K). The model calculations are presented in Figures 5–7.
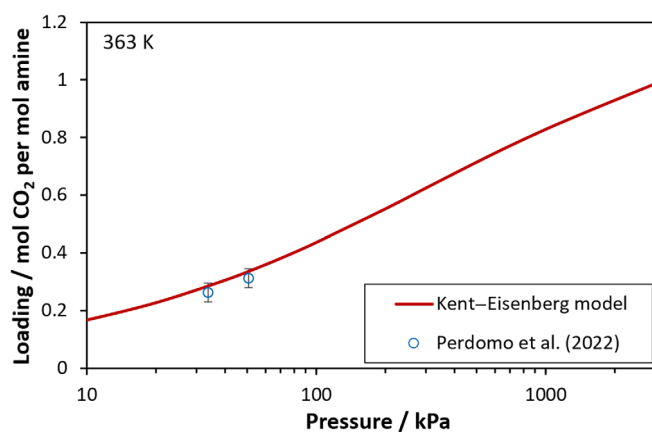
As mentioned in a previous section, CHAP is a diamine (Figure 1) consisting of two amine groups, one that is sterically hindered and, thus, may be considered as non-carbamate amine forming group and one carbamate forming, primary amine group.

In this study, in order to use a minimum number of adjustable parameters, CHAP was modeled assuming a "principle of independent reactivity," that is, that the reactivity of each group does not depend on the potential reaction of the other one. This is an approximation that resembles the Flory's equal reactivity principle, used in polymer chemistry, according to which the reactivity of each group is independent of the chain length and is considered a good approximation for chain lengths higher than approximately four carbon atoms.

As shown in Figure 1, the secondary amine group of CHAP resembles that of MCA. Since the reactivity of each group was assumed independent of its neighbors, the reactivity of the sterically hindered secondary amine group of CHAP can be approximated as equal to the reactivity of MCA. Thus, the $k_{12}$ parameters, obtained for MCA and shown in Table 8, can also be used for the secondary amine group of CHAP. Consequently, in order to apply the model, one should estimate only the parameters of Equation (33) for $k_{11}$ and $k_5$. If those parameters are available, the model can be applied through Equations (26)–(28). If a mixture of two different monoamines is considered, then the calculated loading through Equation (27) denotes the moles of absorbed $CO_2$ per mole of amine molecules. However, in the case of CHAP, which is a diamine consisting of two amine groups, one carbamate forming and one non-carbamate forming group, such equations can also be used. Nevertheless, as mentioned in a previous section, in that case all amine species concentrations showing in
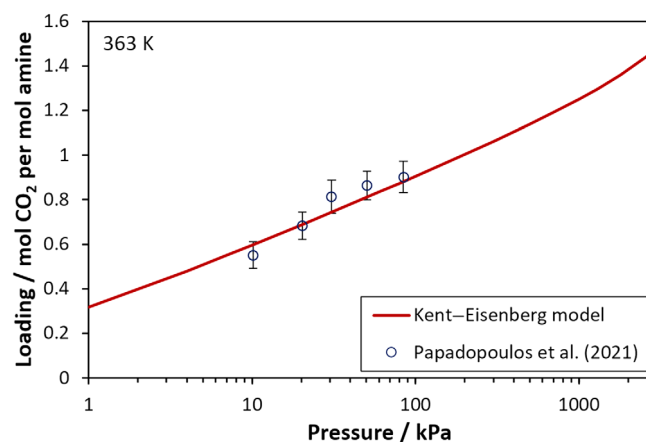


**FIGURE 7** Solubility of $CO_2$ in aqueous MCA solutions at 363 K. Experimental data[11] (symbols) and Kent–Eisenberg correlations (curve)



**FIGURE 8** Solubility of $CO_2$ in aqueous CHAP solutions at 363 K. Experimental data[7] (symbols) and Kent–Eisenberg correlations (curve)

**TABLE 8** Parameters for the empirical equation (33) obtained in this study

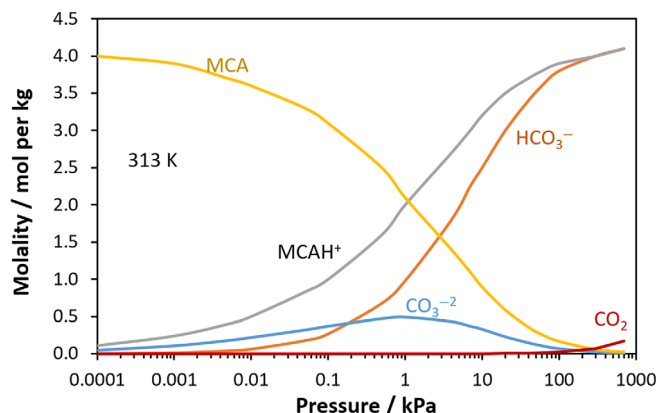| Parameter[a] ($T$ in K) | Units | $A$ | $B$ | $C$ | $D$ | Amine |
|---|---|---|---|---|---|---|
| $k_{12}$ | mol/kg | −7123.29 | – | – | – | MCA and CHAP |
| $k_{11}$ | mol/kg | −4772.54 | – | – | −6.2122 | CHAP |
| $k_5$ | mol/kg | −1517.05 | – | – | 2.1065 | CHAP |

[a]Temperature validity: 313–363 K.

**FIGURE 9**    Model predictions for the liquid phase content of a $CO_2$ loaded MCA solution (4.1 m) at 313.15 K
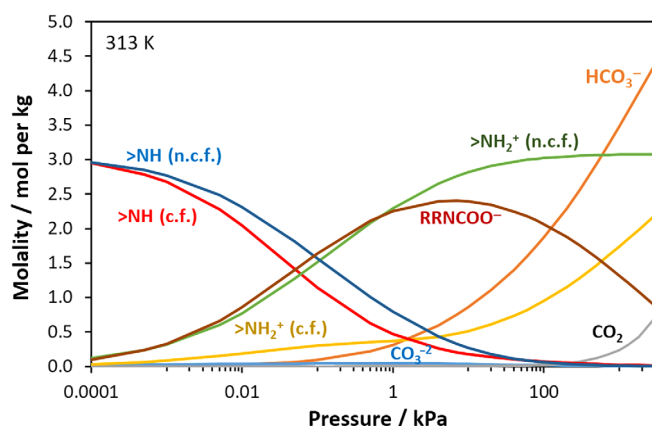


**FIGURE 10**    Model predictions for the liquid phase content of a $CO_2$ loaded CHAP solution (3.1 m) at 313.15 K

Equations (1-28) will denote moles of amine groups and not moles of molecules. Also, the calculated loading from Equation (27) will denote the moles of absorbed $CO_2$ per mole of amine groups (not molecules). Thus, it must be multiplied by two in order to be compared with the experimental data (loading was experimentally measured as moles of $CO_2$ per moles of amine molecules).

Using this approach, the model was applied and the parameters of Equation (33) for $k_{12}$ and $k_5$ were adjusted to the experimental data of this work and that of Papadopoulos et al.[7] To avoid unnecessary empiricism, only two parameters of Equation (33), A and D, were optimized, while the remaining ones were set equal to zero. Therefore, using only two adjustable parameters per equilibrium constant ($k_{12}$ and $k_5$), the model rather satisfactorily correlates the experimental data, presenting an average absolute deviation equal to 2.9% from the used experimental data (for 313, 333, and 363 K). The model calculations are presented in Figures 3, 4, and 8.

Having parameterized the model, the concentration of all species in the liquid phase can be predicted. Such calculations are illustrated in Figures 9 and 10, for MCA and CHAP loaded solutions at 313 K, respectively. It is revealed that the free amine concentration becomes

very low and approaches zero at $CO_2$ partial pressures higher than approximately 100 kPa. At higher $CO_2$ partial pressures, the $CO_2$ solubility increases through molecular $CO_2$ dissolution, as indicated by the respective $CO_2$ curve, and the substantial carbamate hydrolysis, in the case of CHAP, as indicated by the maximum shown in the $RRNCOO^-$ concentration curve.

## 4 | CONCLUSIONS

Aqueous MCA and CHAP solutions were experimentally studied regarding the $CO_2$ solubility at 313 and 333 K and at $CO_2$ partial pressures higher than 50 kPa, using a pressure decay technique. The new high pressure experimental data are in good agreement with the low pressure data, previously obtained from our group using a chemical analysis method. Subsequently, the modified Kent–Eisenberg model was parameterized and used to correlate the available data for such systems. CHAP was modeled assuming a "principle of independent reactivity," that is, that the reactivity of each amine group does not depend on the potential reaction of the other one. Using this approach, the model can be applied to diamines using the relevant equations of amine mixtures. Overall, the model calculations present a satisfactory agreement with the experimental data, presenting an absolute average deviation equal to 5.7% and 2.9%, for MCA and CHAP solutions, respectively.

### AUTHOR CONTRIBUTIONS

**Fragkiskos Tzirakis:** Conceptualization (equal); investigation (equal); methodology (equal); software (equal); validation (equal); visualization (equal); writing – original draft (equal); writing – review & editing (equal). **Athanasios I. Papadopoulos:** Conceptualization (equal); funding acquisition (equal); investigation (equal); project administration (equal); writing – original draft (equal); writing – review and editing (equal). **Panos Seferlis:** Conceptualization (equal); funding acquisition (equal); investigation (equal); project administration (equal); writing – original draft (equal); writing – review and editing (equal). **Ioannis Tsivintzelis:** Conceptualization (equal); investigation (equal); methodology (equal); software (equal); validation (equal); visualization (equal); writing – original draft (equal); writing – review and editing (equal).

### DATA AVAILABILITY STATEMENT

Data available on request from the authors.

### ORCID

*Fragkiskos Tzirakis* https://orcid.org/0000-0001-9062-3321
*Ioannis Tsivintzelis* https://orcid.org/0000-0002-4907-4794

## REFERENCES

1. Bui M, Adjiman CS, Bardow A, et al. Carbon capture and storage (CCS): the way forward. *Energy Environ Sci*. 2018;11(5):1062-1176.

2. Nessi E, Papadopoulos A, Seferlis P. A review of research facilities, pilot and commercial plants for solvent-based post-combustion CO₂ capture: packed bed, phase-change and rotating processes. *Int J Greenh Gas Control*. 2021;111:103474.

3. Zhang S, Shen Y, Shao P, Chen J, Wang L. Kinetics, thermodynamics, and mechanism of a novel biphasic solvent for CO₂ capture from flue gas. *Environ Sci Technol*. 2018;52(6):3660-3668.

4. Papadopoulos AI, Tzirakis F, Tsivintzelis I, Seferlis P. Phase-change solvents and processes for post-combustion CO₂ capture—a detailed review. *Ind Eng Chem Res*. 2019;58(13):5088-5111.

5. Borhani TN, Wang M. Role of solvents in CO₂ capture processes: the review of selection and design methods. *Renew Sustain Energy Rev*. 2019;114:109299.

6. Mangalapally HP, Hasse H. Pilot plant experiments for post combustion carbon dioxide capture by reactive absorption with novel solvents. *Chem Eng Sci*. 2011;66(22):5512-5522.

7. Papadopoulos AI, Perdomo FA, Tzirakis F, et al. Molecular engineering of sustainable phase-change solvents: from digital design to scaling-up for CO₂ capture. *Chem Eng J*. 2021;420:127624.

8. Jessop PG, Heldebrant DJ, Li X, Eckert CA, Liotta CL. Reversible nonpolar-to-polar solvent. *Nature*. 2005;436(7054):1102.

9. Zhang J. *Study On CO₂ Capture Using Thermomorphic Biphasic Solvents with Energy-Efficient Regeneration* (PhD thesis). TU Dortmund; 2013.

10. Kazepidis P, Papadopoulos A, Tzirakis F, Seferlis P. Optimum design of industrial post-combustion CO₂ capture processes using phase-change solvents. *Ind Eng Chem Res*. 2021;175:209-222.

11. Perdomo FA, Khalit SH, Graham EJ, et al. A predictive group-contribution framework for the thermodynamic modelling of CO₂ absorption in cyclic amines, alkyl polyamines, alkanolamines and phase-change amines: new data and SAFT-γ Mie parameters. *Fluid Phase Equilibria*. 2023;566:113635. 10.1016/j.fluid.2022.113635

12. Jeon SB, Cho SW, Lee SS, Jang SY, Oh K. Absorption characteristics of carbon dioxide into an O/W emulsion absorbent containing N-methylcyclohexylamine/2,6 dimethylpiperidine. *J Taiwan Inst Chem Eng*. 2014;45:2673-2680.

13. Tzirakis F, Tsivintzelis I, Papadopoulos AI, Seferlis P. Experimental investigation of phase change amine solutions used in CO₂ capture applications: systems with dimethylcyclohexylamine (DMCA) and N-cyclohexyl-1,3-propanediamine (CHAP) or 3-methylaminopropylamine (MAPA). *Int J Greenh Gas Control*. 2021;109:103353.

14. Tzirakis F, Tsivintzelis I, Papadopoulos AI, Seferlis P. Experimental measurement and assessment of equilibrium behaviour for phase change solvents used in CO₂ capture. *Chem Eng Sci*. 2019;199:20-27.

15. Wang R, Liu S, Li Q, Zhang S, Wang L, An S. CO₂ capture performance and mechanism of blended amine solvents regulated by N-methylcyclohexylamine. *Energy*. 2021;215:119209.

16. Ye Q, Wang X, Lu Y. Screening and evaluation of novel biphasic solvents for energy efficient post-combustion CO₂ capture. *Int J Greenh Gas Control*. 2015;39:205-214.

17. Shen Y, Chen H, Wang L, et al. Two-stage interaction performance of CO₂ absorption into biphasic solvents: mechanism analysis, quantum calculation and energy consumption. *Appl Energy*. 2020;260:114343.

18. Uyan M, Sieder G, Ingram T, Held C. Predicting CO₂ solubility in aqueous N-methyldiethanolamine solutions with ePC-SAFT. *Fluid Phase Equilibria*. 2015;393:91-100.

19. Wangler A, Sieder G, Ingram T, Heiling M, Held C. Prediction of CO₂ and H₂S solubility and enthalpy of absorption in reacting N-methyldiethanolamine/water systems with ePC-SAFT. *Fluid Phase Equilibria*. 2018;461:15-27.

20. Suleman H, Maulud AS, Man Z. Review and selection criteria of classical thermodynamic models for acid gas absorption in aqueous alkanolamines. *Rev Chem Eng*. 2015;31(6):599-639.

21. Rodriguez J, Mac Dowell N, Llovell F, Adjiman CS, Jackson G, Galindo A. Modelling the fluid phase behaviour of aqueous mixtures of multifunctional alkanolamines and carbon dioxide using transferable parameters with the SAFT-VR approach. *Mol Phys*. 2012;110(11–12):1325-1348.

22. Chremos A, Forte E, Papaioannou V, Galindo A, Jackson G, Adjiman CS. Modelling the phase and chemical equilibria of aqueous solutions of alkanolamines and carbon dioxide using the SAFT-γ SW group contribution approach. *Fluid Phase Equilibria*. 2016;407:280-297.

23. Leontiadis K, Tzimpilis E, Aslanidou D, Tsivintzelis I. Solubility of CO₂ in 3-amino-1-propanol and in N-methyldiethanolamine aqueous solutions: experimental investigation and correlation using the CPA equation of state. *Fluid Phase Equilibria*. 2019;500:112254.

24. Tzirakis F, Papadopoulos AI, Seferlis P, Tsivintzelis I. CO₂ absorption capacity of diethylenetriamine (DETA) and triethylenetetramine (TETA) aqueous mixtures: experimental investigation and correlation using the CPA equation of state. *Chem Thermodyn Ther Anal*. 2021;3-4:100017.

25. Kent RL, Eisenberg B. Better data for amine treating. *Hydrocarbon Process*. 1976;55:87-90.

26. Jou F-Y, Mather AE, Otto FD. Solubility of H₂S and CO₂ in aqueous methyldiethanolamine solutions. *Ind Eng Chem Process Des Dev*. 1982;21:539-544.

27. Suleman H, Maulud AS, Fosbøl PL, et al. A review of semi-empirical equilibrium models for CO₂-alkanolamine-H₂O solutions and their mixtures at high pressure. *J Environ Chem Eng*. 2020;9:104713.

28. National Institute of Standards and Technology (NIST). *Isothermal Properties for Carbon Dioxide*. Accessed May 2022. http://webbook.nist.gov/chemistry/

29. Arshad MW, Svendsen HF, Fosbøl FL, von Solms N, Thomsen K. Equilibrium total pressure and CO₂ solubility in binary and ternary aqueous solutions of 2-(diethylamino)ethanol (DEEA) and 3-(methylamino) propylamine (MAPA). *J Chem Eng Data*. 2014;59:764-774.

30. Jou F-Y, Mather AE, Otto FD. The solubility of CO₂ in a 30 mass percent monoethanolamine solution. *Can J Chem Eng*. 1995;73:140-147.

31. Haji-Sulaiman MZ, Aroua MK, Benamor A. Analysis of equilibrium data of CO₂ in aqueous solutions of diethanolamine (DEA), methyldiethanolamine (MDEA) and their mixtures using the modified Kent Eisenberg model. *Trans Inst Chem Eng*. 1998;76:961-968.

32. Edwards T, Maurer G, Newman J, Prausnitz J. Vapor–liquid equilibria in multicomponent aqueous solutions of volatile weak electrolytes. *AIChE J*. 1978;24:966-976.

33. Park SH, Lee KB, Hyun JC, Kim SH. Correlation and prediction of the solubility of carbon dioxide in aqueous alkanolamine and mixed alkanolamine solutions. *Ind Eng Chem Res*. 2002;41:1658-1665.